Full-Duplex vs. Half-Duplex Amplify-and-Forward Relaying: Which is More Energy Efficient in 60 GHz Dual-Hop Indoor Wireless Systems?

Zhongxiang Wei, Xu Zhu, *Senior Member, IEEE,* Sumei Sun, *Senior Member, IEEE,* Yi Huang, *Senior Member, IEEE,* Lihao Dong, *Member, IEEE,* and Yufei Jiang, *Member, IEEE*

***Abstract*—We provide a comprehensive energy efficiency (EE) analysis of the full-duplex (FD) and half-duplex (HD) amplify-and-forward (AF) relay-assisted 60 GHz dual-hop indoor wireless systems, aiming to answer the question of which relaying mode is greener (more energy efficient) and to address the issue of EE optimization. We develop an opportunistic relaying mode selection scheme, where FD relaying with one-stage self-interference cancellation (passive suppression) or two-stage self-interference cancellation (passive suppression + analog cancellation) or HD relaying is opportunistically selected, together with transmission power adaptation, to maximize the EE with given channel gains. A low-complexity joint mode selection and EE optimization algorithm is proposed. We show a counter-intuitive finding that, with a relatively loose maximum transmission power constraint, FD relaying with two-stage self-interference cancellation is preferable to both FD relaying with one-stage self-interference cancellation and HD relaying, resulting in a higher optimized EE. A full range of power consumption sources are considered to rationalize our analysis. The effects of imperfect self-interference cancellation at relay, drain efficiency and static circuit power on EE are investigated. Simulation results verify our theoretical analysis.**

***Index Terms*—Full-duplex, half-duplex, relay, 60 GHz, energy efficiency, optimization**

I. Introduction

Nowadays, wireless communications are required to support much richer multimedia applications, such as uncompressed high definition TV and high speed video downloads. The 60 GHz frequency band, with an extremely large bandwidth of up to 7 GHz, is a promising candidate for high speed indoor wireless networks [1]. However, the 60 GHz transmission requires line-of-sight (LOS) and suffers significant propagation loss due to inherent disadvantages at such high frequency [2]. Also, it is challenging to maintain robust network connectivity at 60 GHz networks. As the wavelength at 60 GHz is only 5 mm, links are easily blocked by obstacles, such as human body and furniture. Applying relay is a leverage to extend network coverage while maintaining robust connectivity [3]. Conventional relays work in half-duplex (HD) mode, while full-duplex (FD) relaying [4], which allows transmitting and receiving at the same frequency and the same time, enables a significant enhancement of system throughput and has attracted much attention. Whereas, it suffers loop interference and requires effective self-interference mitigation [5].

On the other hand, 60 GHz chips generally consume much more power than the chips working at a much lower frequency [6]. Therefore, there is an urgent demand for maintaining high system throughput while limiting energy consumption [7], which has attracted much attention from vendors and researchers, *e.g.*, the IJOIN project [8] and the EARTH project [9]. Energy efficiency (EE), defined as the ratio of system throughput to total power consumption [7], is an important measure of green communication solutions. The EE of the relay-assisted indoor wireless network at 60 GHz should be investigated. It is also interesting to compare the EE achieved by FD relaying with its HD counterpart.

A. Related Work

Self-interference is a critical affecting factor in implementation of FD relaying. There are three main methods for self-interference mitigation: passive suppression (PS), analog cancellation (AC), and digital cancellation (DC) [10].

PS [5] (also referred to as natural isolation) is the first stage of self-interference cancellation, which benefits from antenna placement, directional antenna, antenna polarization or antenna shielding to mitigate self-interference in the propagation domain. Generally, the amount of self-interference can be reduced by more than 40 dB via PS [5] [11]. PS can account for a large portion of the total self-interference cancellation in existing FD designs. At 60 GHz, the performance of PS can be more significant. For example, PS can leverage the path loss (PL) between transmit and receive antennas. At 60 GHz, PL is naturally 20 dB higher than that at 5 GHz and 28 dB higher than that at 2.4 GHz [2]. Also, the self-interference can be easily blocked by obstacles (via antenna shielding) between relay's transmitter and receiver due to very small wavelength at 60 GHz. Using steerable and highly directional antennas is also an efficient and powerful PS method.

In addition to PS, self-interference can be further mitigated by AC, before the signal at the relay goes through low noise amplifier (LNA). The AC cancellation schemes in [12] [13] [14] deploy direct-conversion radio architectures to estimate the self-interference and subtract it at the relay's receiver end. This kind of AC circuit design does not need additional radio

Corresponding author: Xu Zhu.

Zhongxiang Wei, Xu Zhu, Yi Huang, and Yufei Jiang are with the Department of Electrical Engineering and Electronics, the University of Liverpool, Liverpool, UK, L69 3GJ, UK, Email: {hszwei, xuzhu}@liverpool.ac.uk.

Sumei Sun is with the Institute for Infocom Research, A*STAR, Singapore, 138632, Singapore.

Linhao Dong is with the School of Aerospace Engineering, Tsinghua University, Beijing, China, 100084, China.

This work was supported by the University of Liverpool and A*STAR.

frequency (RF) chain at the relay node and thus consumes less power than the AC design in [11] and [15]. With PS and AC of self-interference, the amount of self-interference cancellation can be up to 80 dB [16] [17].

After PS and AC, DC may be applied in digital domain, in the form of digital self-interference canceler or receive beamforming. Digital self-interference canceler requires an equivalent discrete-time baseband model and complex chip design at relay node. It requires accurate estimation of residual self-interference following PS and AC. Therefore, noise is introduced due to estimation errors and circuit distortion. The power of the noise introduced by DC may be higher than the power of the self-interference removed by DC, resulting in a negative effect on the system performance [11]. Meanwhile, receive beamforming is only applicable in multi-input multi-output (MIMO) FD systems [18] [19]. Therefore, PS only or PS and AC together (referred to as PSAC) are considered to be more suitable self-interference cancellation approaches for amplify-and-forward (AF) FD relaying systems [17].

The previous research on FD relaying has focused on improving throughput [20], or finding the rate gain region (the rate gain region is defined as the region where one relaying mode outperforms another mode in terms of throughput) with specific self-interference mitigation technique [21]. The EEs of FD and HD relaying have not been investigated. A power consumption model was presented in [22] for HD relay-assisted 60 GHz systems. It did not consider FD mode nor static circuit power, which is actually comparable with the transmission power in indoor environments. In the FP7 EARTH [9] project, the power consumption of different types of communication nodes was investigated. For a small-scale base station (such as relay, femto or pico cell base station), its power amplifier (PA) power accounts for 40%$\sim$47% of the total power [9]. Thus the total power consumption mainly includes two parts in indoor environment: PA power and circuit power. The circuit power consumption modeled in [23] is oversimplified and inaccurate due to lack of power consumption details. The circuit power modeled in [24] and [25] contains various power consumption sources including digital-to-analog converter (DAC), mixer, LNA, analog-to-digital converter (ADC), *etc*. However, the circuit power was assumed to be fixed, neglecting the fact that part of the circuit power is dependent on the throughput state. On the other hand, R. Bolla *et al*., [7] explored various perspectives of power consumption and energy saving operations, such as dynamic adaptation and sleeping/standby. In [26] and [27], the EE of direct transmission (without relay) was investigated. In [26], the EE was investigated for orthogonal frequency division multiple access (OFDMA) networks. Li *et al*., [27] presented multiple transmission schemes to minimize energy consumption for wireless video transmission. [28] and [29] presented the analysis of the EE of HD relaying systems. [28] showed how HD relays should be positioned to outperform direct transmission in terms of EE. In [29], a multipath routing algorithm was presented for an HD relaying system, where only the transmission power is included into the power consumption model. There lacks an analysis of the EE of FD relaying in the literature.

B. Summary of Contributions

In this paper, we provide a comprehensive EE analysis of dual-hop FD AF relay-assisted orthogonal frequency division multiplexing (OFDM) systems, in comparison to its HD relaying counterpart. Our work is different in the following aspects.

- To the best of our knowledge, this is the first work to investigate the EE of the FD relaying system and to compare it with its HD relaying counterpart. It is shown that with given transmission power at the source, the FD relaying system can be more energy efficient than the HD relaying system.
- The EE gain regions between FD (PSAC), FD (PS) and HD, where one relaying mode outperforms another mode in terms of EE, are clearly defined. It is shown that FD with two-stage self-interference cancellation (PSAC) can be even more energy efficient than FD with one-stage interference cancellation (PS only) as well as HD, if the transmission power is relatively high and satisfies certain conditions. This enables opportunistic relaying mode selection among FD (PSAC), FD (PS) and HD to optimize the EE under a maximum transmission power constraint.
- It is proved that the EE is strictly quasi-concave or mono-increasing with respect to the transmission power, under a maximum transmission power constraint. A low-complexity algorithm is proposed to optimize the EE.
- A full range of power consumption sources is considered in our power consumption model and their effects on EE are discussed. In particular, the powers consumed by the relay node and self-interference cancellation are considered, which were absent from the previous work on power consumption modeling. The impact of imperfect self-interference cancellation is also considered in our analysis.

This paper is organized as follows. In Section II, the system model is presented. Analysis of the throughput and power consumption is analyzed in Section III. EE optimization is presented in Section IV. The numerical results and conclusions are shown in Sections V and VI, respectively.

II. System Model

We consider a 3-node dual-hop AF relaying system. AF relay is employed because it requires relatively simple signal processing and low operational power [30]. The block diagram of the FD AF relay-assisted system is illustrated in Fig. 1, where PAs are employed at the transmitters of the source and the relay and cascaded LNAs are placed at the receivers of relay and the destination. It is assumed that the destination cannot hear the source directly due to high attenuation at 60 GHz [1] [3], and the relay is positioned in the middle of the source-destination link to maintain a high throughput [31]. The relay in FD mode transmits and receives at the same time and frequency, causing self-interference to the receiver from its transmitter. To reduce the self-interference, PS and AC are applied, as shown in Fig. 1. DC is not considered in this model due to high complexity and performance limitations (PS and AC only can be sufficiently effective for AF FD relaying [17]).

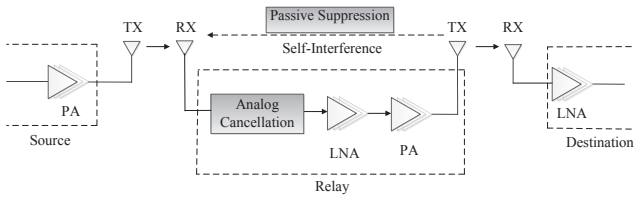

Fig. 1. Block diagram of a simplified FD AF relay-assisted system.

Let α denote the total amount of self-interference cancellation on each subcarrier, which is defined as the ratio of the self-interference powers before and after suppression/cancellation. PS includes directional antenna and antenna shielding. An absorptive shielding (or absorber) between the relay's transmit antenna and receive antenna can block self-interference by around 10 dB in addition to directional antenna [5]. Let α_{PS} denote the total amount of self-interference canceled by PS. The AC circuit design in [14] is adopted due to its simple implementation and no requirement for baseband signal at relay node. Its self-interference cancellation amount is denoted by α_{AC}.

With a frequency-selective fading channel, the channel frequency response and the allocated power are different across subcarriers. Ideally, the self-interference mitigation should be operated subcarrier by subcarrier. However, it is impossible for PS and also imposes extremely high complexity for AC. Therefore, for both PS and AC, self-interference cancellation is frequency-flat cancellation practically: the self-interference cancellation amount is identical across all subcarriers. Thus, $\alpha = \alpha_{PS}$ in FD (PS) and $\alpha = \alpha_{PS} + \alpha_{AC}$ in FD (PSAC). In general, α_{PS} = 40 dB or more can be achieved by PS alone, and $\alpha_{AC} = 20{\sim}40$ dB [12] [14].

We assume OFDM transmission with N subcarriers. Let $h_{SR,n}$, $h_{RD,n}$ and $h_{RR,n}$ denote the channel frequency responses of links source-to-relay (S-R), relay-to-destination (R-D) and relay-to-relay (R-R) on subcarrier n, respectively. Also let l_{SR}, l_{RD} and l_{RR} denote the PLs of links S-R, R-D and R-R, respectively. The channels of the S-R and R-D links are modeled as Rician fading. It is widely used for 60 GHz channel modeling [32] [33], especially with directional antenna and beamforming, which are essential for 60 GHz frequency band to combat high PL. The Saleh-Valenzuela (S-V) model is similar to the Rician model if the direct link is not blocked and its strength is relatively high compared to other non-direct components [34]. The self-interference channel is modeled as Rayleigh fading as the LOS between the transmitter and the receiver of the relay can be easily blocked by antenna shielding due to very small wavelength at 60 GHz. Applying narrow beamwidth antenna also reduces the LOS signal strength between relay's transmitter and receiver due to the main lobe of the relay's directional transmit antenna pointing to the destination. The self-interference waves are collected from the reflected waves [34].

Assume that the PAs have equal power gain of β, and the LNAs have the same gain G and noise figure F each [22]. Let $s_n[k]$ denote the transmitted signal at the source on subcarrier n in time slot k, and $P_{s,n}$ is the allocated transmission power at the source. Similarly, define $t_n[k]$ as the transmitted signal at the relay on subcarrier n in time slot k. $z_{R,n}[k]$ and $z_{D,n}[k]$ denote complex additive white Gaussian noise (AWGN) elements on subcarrier n introduced at the relay and destination, respectively, with zero mean and variance σ^2.

With residual self-interference, the received signal at the relay node on subcarrier n in time slot k is expressed as:

$$r_n[k] = h_{SR,n}\sqrt{l_{SR}P_{s,n}}s_n[k] + h_{RR,n}\sqrt{\frac{1}{\alpha}}t_n[k-\tau] + z_{R,n}[k], \tag{1}$$

where τ (≥ 1) is the integer symbol processing delay, which is typically long enough to guarantee that the symbol transmitted at the relay is uncorrelated with the symbol received simultaneously [35]. The signal received at the relay passes through cascaded LNAs and PA. Thus, the transmitted signal $t_n[k]$ from the relay is given by

$$\begin{aligned} t_n[k] = \sqrt{\beta G}\Big(&h_{SR,n}\sqrt{l_{SR}P_{s,n}}s_n[k] + \\ &h_{RR,n}\sqrt{\frac{1}{\alpha}}t_n[k-\tau] + \sqrt{F}z_{R,n}[k]\Big). \end{aligned} \tag{2}$$

At the destination, the received signal is processed by LNAs again and is collected as

$$\begin{aligned} y_n[k] =& h_{RD,n}\sqrt{\beta G^2 l_{RD}}\Big(h_{SR,n}\sqrt{l_{SR}P_{s,n}}s_n[k] \\ &+ h_{RR,n}\sqrt{\frac{1}{\alpha}}t_n[k-\tau] + \sqrt{F^2}z_{R,n}[k]\Big) \\ &+ \sqrt{GF}z_{D,n}[k]. \end{aligned} \tag{3}$$

III. THROUGHPUT AND POWER CONSUMPTION ANALYSIS

EE involves both system throughput and total power consumption. Hereby, we analyze the throughout and power consumption in separate subsections.

A. Throughput Analysis

The received signal at the destination is rewritten as

$$\begin{aligned} y_n[k] =& \underbrace{h_{RD,n}\sqrt{\beta G^2 l_{RD}}h_{SR,n}\sqrt{l_{SR}P_{s,n}}s_n[k]}_{\text{desired signal}} \\ &+ \underbrace{h_{RD,n}\sqrt{\beta G^2 l_{RD}}h_{RR,n}\sqrt{\frac{1}{\alpha}}t_n[k-\tau]}_{\text{self-interference}} \\ &+ \underbrace{h_{RD,n}\sqrt{\beta G^2 l_{RD}}\sqrt{F^2}z_{R,n}[k] + \sqrt{GF}z_{D,n}[k]}_{\text{equivalent noise}}, \end{aligned} \tag{4}$$

where the equivalent noise consists of the noise introduced at the relay and destination. Let Γ_n denote the signal-to-interference-and-noise ratio (SINR) on subcarrier n at the destination. Define $g_{1,n} = \beta G^2 |h_{SR,n}|^2 l_{SR} |h_{RD,n}|^2 l_{RD}$, $g_{2,n} = GF + \beta G^2 F^2 |h_{RD,n}|^2 l_{RD}$, $g_{3,n} = \beta^2 G^3 F^3 |h_{RD,n}|^2 l_{RD} |h_{RR,n}|^2$ and $g_{4,n} = \beta^2 G^3 |h_{SR,n}|^2 l_{SR} |h_{RD,n}|^2 l_{RD} |h_{RR,n}|^2$.

According to (4), the SINR on subcarrier n at the destination with FD relaying can be derived as

$$\Gamma_{FD,n} = \frac{g_{1,n}P_{s,n}}{g_{2,n}\sigma^2 + P_{I,n}/\alpha}, \tag{5}$$

where $P_{I,n} = g_{3,n}\sigma^2 + g_{4,n}P_{s,n}$ represents the power of the self-interference, $g_{2,n}\sigma^2$ is the power of the equivalent noise and $g_{1,n}P_{s,n}$ is the power of the desired signal. Unlike [21] which assumed a bidirectional P-to-P FD system, in our system model, the noise introduced at the relay node and the residual self-interference after cancellation are forwarded to the destination, which can be observed from (4) and (5). The overall throughput of FD is given by

$$T_{FD} = \sum_{n=1}^{N} \frac{W}{N} \log_2(1 + \Gamma_{FD,n}). \tag{6}$$

For HD relaying transmission, the SINR $\Gamma_{HD,n}$ is calculated by setting the self-interference related elements in (5) to 0 and 1/2 is added before the log function in (6) due to orthogonal time transmission.

To outperform HD in terms of throughput on subcarrier n, the following equation should be satisfied by FD:

$$\frac{W}{N} \log_2(1 + \Gamma_{FD,n}) > \frac{W}{2N} \log_2(1 + \Gamma_{HD,n}). \tag{7}$$

Substituting (5) into (7), we get

$$\alpha > \frac{g_{3,n}p_{s,n} + g_{4,n}\sigma^2}{\sqrt{(g_{1,n}p_{s,n} + g_{2,n}\sigma^2)(g_{2,n}\sigma^2)}}. \tag{8}$$

Equation (8) indicates that the required self-interference cancellation amount making FD outperform HD in terms of throughput on subcarrier n. It is obvious that a higher cancellation amount can satisfy (8) more easily. To increase the self-interference cancellation amount, many cancellation schemes have been proposed [5] [11] [12] [13] [14]. With proper self-interference cancellation design, the power of self-interference can be lower or even negligible compared to noise power. As shown from (8), higher power gain β at amplifier requires more self-interference cancellation amount α at relay node. It is because improving power gain can improve the SINR at the second hop R-D, but corrupt the SINR at the first hop S-R. The effect of amplifier power gain β on the first hop is much more significant than its effect on the second hop because the distance between relay's transmitter and receiver is much shorter than the distance between relay's transmitter and destination's receiver. Therefore, higher self-interference cancellation amount α is required for a higher value of β. Also, LNAs at relay are placed at the front-end of relay's receiver. Normally, the effect of noise from subsequent stages (*e.g.*, noise introduced at the destination) is reduced by the gain of the relay's LNAs in a dual-hop network. Therefore, high gain LNA is preferred at the relay (the noise figure is considered approximately irrelevant to the power gain of LNA by good LNA design). However, the boosted signal by LNA is treated as self-interference to the relay's receiver when it is transmitted to the destination. Therefore, higher self-interference cancellation amount α is needed to compensate for the effect of a higher valued G, as can be seen from (8).

B. Power Consumption Analysis

Assume continuous data transmission, so that the power consumption is in active mode. We adopt the typical power consumption model for short-range or indoor communications [9] [26], where the total power consumption contains two main parts, circuit power P_c and PA power P_{PA}. The circuit power consumption includes the power consumed by all circuit blocks along the signal path while the PA power is consumed by both source and relay. The power consumption for AC, P_{AC}, is also considered if the relay works in FD mode.

PA Power: The total PA power includes the transmission power and the dissipated power of PAs at both source and relay, given by

$$P_{PA} \approx \sum_{n=1}^{N} \frac{P_{s,n}}{\omega} \left(1 + \beta G |h_{SR,n}|^2 l_{SR}\right), \tag{9}$$

where ω is the drain efficiency [36]. The power allocated onto subcarrier n is a portion of the total transmission power P_s, that is, $P_{s,n} = \lambda_n P_s$, where $0 \le \lambda_n \le 1$ and $\sum_{n=1}^{N} \lambda_n = 1$. Defining $\tilde{\lambda}_n = \lambda_n \left(1 + \beta G |h_{SR,n}|^2 l_{SR}\right)$, (9) can be rewritten as

$$P_{PA} = \left(\frac{P_s}{\omega}\right) \sum_{n=1}^{N} \tilde{\lambda}_n. \tag{10}$$

Circuit Power: The circuit power P_c includes the power consumed by all circuit blocks along the signal path, which can be divided into static circuit power, $P_{c,sta}$, and dynamic circuit power, $P_{c,dyn}$ [26]. The former can be formulated as a fixed value [25], while the dynamic circuit power is closely related to the throughput state [37] . A well-accepted model of dynamic circuit power is $P_{c,dyn} = \varepsilon T$, where the constant ε denotes the power consumption per unit data rate [26]. Also, relay's circuit power is non-negligible in indoor environment [38]. Thus, the total circuit power is given by

$$P_c = P_{c,sta} + \varepsilon T. \tag{11}$$

Power for Self-Interference Cancellation: Applying PS actually does not consume additional power, however, the power consumed by AC is non-negligible. Besides, the power consumed by the involved chip components, such as attenuator and splitter, are not related to the throughput state [13] [14], and therefore the power consumed by AC, P_{AC}, is regarded as a constant. Using (10) and (11), the total power consumption is formulated as

$$P = \left(\frac{P_s}{\omega}\right) \sum_{n=1}^{N} \tilde{\lambda}_n + \varepsilon T + P_{c,sta} + \xi P_{AC}, \tag{12}$$

where $\xi = 1$ for FD (PSAC) relaying and $\xi = 0$ for FD (PS) relaying and HD relaying.

IV. ENERGY EFFICIENCY OPTIMIZATION

EE is calculated as the ratio of the system throughput to the total power consumption, which are derived in Section III:

$$\eta = \frac{T}{P}. \tag{13}$$

In conventional cellular networks, circuit power dominates the power consumption and the consumed transmission power is negligible. As illustrated in [39], the circuit power of base station is dominant and could be up to 3700 W in a macro-cellular network. Thus, its EE can be approximated by $\eta = \frac{T}{P_{c,sta}+\varepsilon T_+ \xi P_{AC}}$. Higher EE is pursued by setting the transmission power as high as possible to achieve a high throughput. In 60 GHz indoor systems, however, higher throughput may lead to lower EE due to enhanced transmission power, which cannot be neglected in total power consumption.

Our objective is to optimize the instantaneous EE η, *i.e.,*

$$Max \;\; \eta \tag{14}$$

$$Subject\ to \;\; P_s \leq P_{max}. \tag{15}$$

In Subsection IV-A, we discuss how to optimize EE by transmission power adaptation at source under a maximum transmission power constraint. In Subsection IV-B, we research the EE gain regions between FD (PSAC), FD (PS) and HD relaying modes. With opportunistic relaying mode selection and transmission power adaptation, EE is maximized. Some parametric effects on EE gain regions are discussed in Subsection IV-C.

A. Transmission Power Adaptation for EE Optimization

Theorem 1: In AF FD/HD relay-assisted OFDM systems with good self-interference cancellation, EE η is strictly quasi-concave or mono-increasing with respect to transmission power $P_s \in (0, P_{max}]$.

Proof of Theorem 1: See APPENDIX A.

According to Theorem 1, under a transmission power constraint P_{max}, there is one and only one globally/locally optimal transmission power in terms of EE η, which can be found by calculating the gradient of η in terms of transmission power P_s. We propose a so-called gradient calculation (GC) algorithm to optimize EE η by adjusting the total transmission power, as shown in Algorithm 1.

The proposed GC algorithm relies on $\frac{\partial \eta}{\partial P_s}$. It is hard to derive a closed-form expression of $\frac{\partial \eta}{\partial P_s}$, however, we can use the definition of derivative to get the value of $\frac{\partial \eta}{\partial P_s}$ at any given transmission power, as shown in APPENDIX B. With the proposed GC algorithm and feasible calculation of $\frac{\partial \eta}{\partial P_s}$, the globally/locally optimal transmission powers in the region of $P_s \in (0, P_{max}]$ can be found for FD (PSAC), FD (PS) and HD, respectively.

B. EE Gain Regions and Opportunistic Relaying Mode Selection

In Subsection IV-A, the GC algorithm is proposed to optimize the EEs of FD (PSAC), FD (PS) and HD relaying modes, respectively. The three modes may have different optimized EE values due to different throughputs and power consumptions. In this subsection, we first discuss the EE gain regions between the three relaying modes, which serve opportunistic relaying mode selection. It is different from the work in [35] and [40] on opportunistic relaying mode selection, which were based on system throughput. Then we combine opportunistic relaying mode selection with transmission power adaptation to obtain the maximum system EE.

Algorithm 1 GC Algorithm for Transmission Power Adaptation

if $\frac{\partial \eta}{\partial P_s}|_{P_{max}} \geq 0$ **then**
  EE is mono-increasing in the range of $P_s \in (0, P_{max}]$.
  return $\eta^* = \eta(P_{max})$.
else
  EE is quasi-concave in the range of $P_s \in (0, P_{max}]$.
  Initialize the left bound $P_L = 0$, and the right bound $P_R = P_{max}$.
  while $|\frac{\partial \eta}{\partial P_s}|_P| < \delta$ (δ is a precision factor) **do**
    $P = \frac{P_L + P_R}{2}$.
    Calculate $a = \frac{\partial \eta}{P_s}\big|_{P_L}$ and $b = \frac{\partial \eta}{P_s}\big|_{P}$.
    if $a \cdot b \geq 0$ **then**
      $P_L = P$.
    else
      $P_R = P$.
    end if
  end while
  return $\eta^* = \eta(P)$.
end if

Substituting (6) and (12) into (13) yields the EE of FD (PSAC) as:

$$\eta_{FD(PSAC)} = \frac{T_{FD(PSAC)}}{\left(\frac{P_s}{\omega}\right)\sum_{n=1}^{N}\tilde{\lambda}_n + \varepsilon T_{FD(PSAC)} + P_{c,sta} + P_{AC}}. \tag{16}$$

The EE of FD (PS) is given by

$$\eta_{FD(PS)} = \frac{T_{FD(PS)}}{\left(\frac{P_s}{\omega}\right)\sum_{n=1}^{N}\tilde{\lambda}_n + \varepsilon T_{FD(PS)} + P_{c,sta}}. \tag{17}$$

Similarly, the EE of HD is given by

$$\eta_{HD} = \frac{T_{HD}}{\left(\frac{P_s}{\omega}\right)\sum_{n=1}^{N}\tilde{\lambda}_n + \varepsilon T_{HD} + P_{c,sta}}. \tag{18}$$

Similarly to the rate gain region defined in [20], the EE gain region is defined as the region in which one relaying mode outperforms another mode in terms of EE. In the following, we compare the EEs of FD (PSAC), FD (PS) and HD relaying modes with given transmission power P_s, which is constrained by a maximum transmission power P_{max}. The differences between the EEs of the three relaying modes are provided in APPENDIX C.

1) FD (PSAC) vs. FD (PS)

It is obvious that the system throughput of FD (PSAC) is always higher than that of FD (PS), *i.e.,* $T_{FD(PS)} < T_{FD(PSAC)}$, at the cost of additional power consumption on AC operation. According to (23) in APPENDIX C, if the value of $(\frac{P_s}{\omega}\sum_{n=1}^{N}\tilde{\lambda}_n + P_{c,sta})(\frac{T_{FD(PSAC)}}{T_{FD(PS)}} - 1) < P_{AC}$, then $\eta_{FD(PSAC)} - \eta_{FD(PS)} < 0$, *i.e.,* FD (PS) is more energy efficient than FD (PSAC). If the transmission power P_s keeps increasing, the value of $\left(\frac{P_s}{\omega}\sum_{n=1}^{N}\tilde{\lambda}_n + P_{c,sta}\right) \cdot \left(\frac{T_{FD(PSAC)}}{T_{FD(PS)}} - 1\right)$ may exceed the value of P_{AC}, leading to

$$P_s^{\dagger,1} = \begin{cases} \dfrac{\omega}{\sum_{n=1}^{N}\tilde{\lambda}_n}\left(\dfrac{P_{AC}}{\frac{T_{FD(PSAC)}}{T_{FD(PS)}}-1} - P_{c,sta}\right), & \frac{T_{FD(PSAC)}}{T_{FD(PS)}} < \frac{P_{AC}}{P_{c,sta}}+1 \\ 0, & \frac{T_{FD(PSAC)}}{T_{FD(PS)}} \geq \frac{P_{AC}}{P_{c,sta}}+1. \end{cases} \tag{19}$$

$$P_s^{\dagger,2} = \begin{cases} \dfrac{\omega}{\sum_{n=1}^{N}\tilde{\lambda}_n}\left(\dfrac{P_{AC}}{\frac{T_{FD(PSAC)}}{T_{HD}}-1} - P_{c,sta}\right), & 1 < \frac{T_{FD(PSAC)}}{T_{HD}} < \frac{P_{AC}}{P_{c,sta}}+1 \\ 0, & \frac{T_{FD(PSAC)}}{T_{HD}} \geq \frac{P_{AC}}{P_{c,sta}}+1. \end{cases} \tag{20}$$

$\eta_{FD(PSAC)} - \eta_{FD(PS)} > 0$. This implies that FD (PSAC) becomes more energy efficient than FD (PS) when the transmission power is higher than a crossing power $P_s^{\dagger,1}$, which is calculated as (19).

Lemma 1: Under a maximum transmission power constraint P_{max}, any transmission power P_s in the range of $P_s \in (P_s^{\dagger,1}, P_{max}]$ enables FD (PSAC) to outperform FD (PS) in terms of EE.

By considering (19) and Lemma 1 together, the EE gain region for FD (PSAC) outperforming FD (PS) is given as $P_s \in (P_s^{\dagger,1}, P_{max}]$, and the EE gain region for FD (PS) outperforming FD (PSAC) is $P_s \in (0, P_s^{\dagger,1})$. If $P_{max} < P_s^{\dagger,1}$, FD (PS) is always more energy efficient than FD (PSAC) in the range of $P_s \in (0, P_{max}]$.

2) FD (PSAC) vs. HD

According to (24) in APPENDIX C, the sign of $\eta_{FD(PSAC)} - \eta_{HD}$ is the same as the sign of $\left(\frac{P_s}{\omega}\sum_{n=1}^{N}\tilde{\lambda}_n + P_{c,sta}\right)\left(\frac{T_{FD(PSAC)}}{T_{HD}}-1\right) - P_{AC}$. If $T_{HD} \geq T_{FD(PSAC)}$ holds within the feasible range of $P_s \in (0, P_{max}]$, $\eta_{FD(PSAC)} < \eta_{HD}$ is readily derived. If $T_{HD} < T_{FD(PSAC)}$, which occurs commonly, the value of $(\frac{P_s}{\omega}\sum_{n=1}^{N}\tilde{\lambda}_n + P_{c,sta})(\frac{T_{FD(PSAC)}}{T_{HD}}-1)$ may be smaller than that of P_{AC}. Thus, the crossing transmission power for FD (PSAC) outperforming HD is calculated as (20).

Lemma 2: Under a maximum transmission power constraint P_{max}, any transmission power P_s in the range of $P_s \in (P_s^{\dagger,2}, P_{max}]$ enables FD (PSAC) to outperform HD in terms of EE.

By considering (20) and Lemma 2 together, the EE gain region for FD (PSAC) outperforming HD is given by $P_s \in (P_s^{\dagger,2}, P_{max}]$, and the EE gain region for HD outperforming FD (PSAC) is $P_s \in (0, P_s^{\dagger,2})$. If $P_{max} < P_s^{\dagger,2}$, HD is always more energy efficient than FD (PSAC) in the range $P_s \in (0, P_{max}]$.

Specially, with near-perfect self-interference cancellation, the throughput of FD (PSAC) approximately doubles that of HD, *i.e.,* $T_{FD(PSAC)} \approx 2T_{HD}$ [17]. Hence, (20) reduces to

$$P_s^{\dagger,2} = \frac{\omega}{\sum_{n=1}^{N}\tilde{\lambda}_n}\left(P_{AC} - P_{c,sta}\right). \tag{21}$$

In general, the power consumed by AC is lower than the static circuit power consumption by proper design of the AC circuit. That is, $P_{AC} < P_{c,sta}$ [6] [14] and $P_s^{\dagger,2} = 0$. Thus, we can derive Remark 1 below.

Remark 1: With near-perfect self-interference cancellation at the relay and $T_{FD(PSAC)} \approx 2T_{HD}$, FD (PSAC) outperforms HD in terms of EE, given any transmission power P_s in the range of $P_s \in (0, P_{max}]$.

3) FD (PS) vs. HD

According to (26) in APPENDIX C, FD (PS) outperforms HD in terms of EE if $T_{FD(PS)} > T_{HD}$. By (19) and (20), $T_{FD(PS)} > T_{HD}$ is readily obtained if $P_s^{\dagger,1} > P_s^{\dagger,2}$ holds.

The EE gain regions and the corresponding conditions analyzed above are summarized in TABLE I. It provides clear guidance on opportunistic relaying selection, that is, the relaying mode achieving the highest EE is selected given transmission power and channel gains. The combination of opportunistic relaying mode selection and transmission power adaptation is described in Algorithm 2.

Algorithm 2 EE Optimization with Opportunistic Relaying Mode Selection and Transmission Power Adaptation

1: Calculate $T_{FD(PSAC)}, T_{FD(PS)}$ and T_{HD} with transmission power $P_s = P_{max}$.
2: **if** $T_{HD} > T_{FD(PSAC)}$ **then**
3: Call the GC algorithm for HD.
4: **return** $\eta^* = \eta^*_{FD(HD)}$.
5: **else**
6: Calculate $P_s^{\dagger,1}$ and $P_s^{\dagger,2}$ according to (19) and (20), respectively.
7: **In case:** $P_{max} > P_s^{\dagger,1} > P_s^{\dagger,2}$
8: Call the GC algorithm for FD (PSAC) and FD (PS).
9: **Return** $\eta^* = max\{\eta^*_{FD(PSAC)}, \eta^*_{FD(PS)}\}$.
10: **In case:** $P_s^{\dagger,2} > P_s^{\dagger,1} > P_{max}$ or $P_s^{\dagger,2} > P_{max} > P_s^{\dagger,1}$
11: Call the GC algorithm for HD only.
12: **Return** $\eta^* = \eta^*_{HD}$.
13: **In case:** $P_{max} > P_s^{\dagger,2} > P_s^{\dagger,1}$
14: Call the GC algorithm for FD (PSAC) and HD.
15: **Return** $\eta^* = max\{\eta^*_{FD(PSAC)}, \eta^*_{HD}\}$.
16: **In case:** $P_s^{\dagger,1} > P_{max} > P_s^{\dagger,2}$ or $P_s^{\dagger,1} > P_s^{\dagger,2} > P_{max}$
17: Call the GC algorithm for FD (PS) only.
18: **Return** $\eta^* = \eta^*_{FD(PS)}$.
19: **end if**

C. Parametric Effects on EE Gain Regions

At 60 GHz, a maximum PA drain efficiency of $\omega = 25\%$ can be achieved [36], which is lower than the drain efficiency at a lower frequency, *e.g.*, $\omega = 50\%$ at 2.4 GHz.

TABLE I. Summary of EE Gain Regions and the Corresponding Conditions

	EE Comparison	Conditions
Case 1	$\eta_{HD} < \eta_{FD(PS)} < \eta_{FD(PSAC)}$	$P_s^{\dagger,2} < P_s^{\dagger,1}$ and $P_s \in (P_s^{\dagger,1}, P_{max}]$
Case 2	$\eta_{HD} < \eta_{FD(PSAC)} < \eta_{FD(PS)}$	$P_s^{\dagger,2} < P_s^{\dagger,1}$ and $P_s \in (P_s^{\dagger,2}, min\{P_s^{\dagger,1}, P_{max}\})$
Case 3	$\eta_{FD(PS)} < \eta_{HD} < \eta_{FD(PSAC)}$	$P_s^{\dagger,1} < P_s^{\dagger,2}$ and $P_s \in (P_s^{\dagger,2}, P_{max}]$
Case 4	$\eta_{FD(PS)} < \eta_{FD(PSAC)} < \eta_{HD}$	$P_s^{\dagger,1} < P_s^{\dagger,2}$ and $P_s \in (P_s^{\dagger,1}, min\{P_s^{\dagger,2}, P_{max}\})$
Case 5	$\eta_{FD(PSAC)} < \eta_{FD(PS)} < \eta_{HD}$	$P_s^{\dagger,1} < P_s^{\dagger,2}$ and $P_s \in (0, P_s^{\dagger,1})$
Case 6	$\eta_{FD(PSAC)} < \eta_{HD} < \eta_{FD(PS)}$	$P_s^{\dagger,2} < P_s^{\dagger,1}$ and $P_s \in (0, P_s^{\dagger,2})$

According to Lemmas 1 and 2, low drain efficiency ω results in $P_s^{\dagger,1}$ and $P_s^{\dagger,2}$ approaching 0. Also, a higher static circuit power is required for 60 GHz than a lower frequency [6]. If the circuit static power is so large that $P_{c,sta} > \frac{P_{AC}}{T_{FD(PSAC)}/T_{FD(PS),HD}-1}$, $P_s^{\dagger,1} = 0$ or $P_s^{\dagger,2} = 0$ is obtained, which means that the static circuit power dominates the total power consumption, and that FD (PSAC) outperforms FD (PS) or HD in terms of EE with any transmission power. Therefore, Remark 2 below can be drawn.

Remark 2: Low PA drain efficiency or high static circuit power enables a large range of transmission power, over which FD (PSAC) relay systems achieve a higher EE than FD (PS) or HD relaying systems.

Existing PS schemes do not consume additional power. Therefore, improving its self-interference cancellation amount α_{PS} can improve the EEs of both FD (PS) and FD (PSAC). For the cancellation operation at the second stage, generally, better AC performance needs more accurate and complex circuit design, which consumes higher power P_{AC} and could reduce the EE of FD (PSAC) over FD (PS). By proper design, such as effective antenna shielding or highly directional antenna, the performance of PS could be sufficient enough [5]. In this case, applying AC does not improve the throughput significantly as the residual self-interference after PS is already little. Thus, Remark 3 is derived below.

Remark 3: If the self-interference cancellation amount of PS is sufficient, applying additional AC may reduce EE.

V. Numerical Results

We use numerical results to verify our analysis in Section IV. The simulation setup [22] [41] is shown in TABLE II. The PL model measured in [41] is adopted, as $l = 68 + 10\theta log_{10}(d/d_0)$, where θ is the PL exponent, d is the distance between two nodes, and d_0 is reference distance, which is normally set to 1 m in indoor environment. The total self-interference cancellation amounts of FD (PSAC), FD (PS) are set to α = 60 dB and 40 dB, respectively, which are within the reasonable range of cancellation amount as discussed in Subsection I-A and Section II.

Fig. 2 demonstrates the average system throughput achieved with different transmission powers. The throughputs achieved by two FDs are much higher than the throughput achieved by the HD relaying. With a transmission power of 40 mW, the throughputs achieved by FD (with perfect interference cancellation), FD (PSAC, α = 60 dB), FD (PS, α = 40 dB), and HD are approximately 1.92 Gbps, 1.9 Gbps, 1.3 Gbps and 0.96 Gbps, respectively. As expected, with good interference cancellation, FD (PSAC) achieves a throughput that is approximately twice as high as that of HD. The ratio between the throughputs of FD (PSAC) and FD (PS) is around 1.4.

TABLE II. Simulation Setup

Central carrier frequency f_c	60 GHz
Bandwidth W	2640 MHz
Number of subcarriers	512
AWGN power spectral density	-174 dBm/Hz
Distance between source and relay	5 m
Distance between relay and destination	5 m
Distance between source and destination	10 m
Power gain of each LNA G	10.5 dB
Noise figure of each LNA F	5.5 dB
Number of cascaded LNAs at relay and destination	3
Power gain of PA	16 dB
PL exponent θ	3
The ratio of LOS to NLOS for Rician channel	10 dB
Static power consumption $P_{c,sta}$	200 mW
Dynamic circuit factor ε	50 mW/Gbps
Drain efficiency of PA ω	25%
Cancellation amount α	α_{PS} = 40 dB, α_{AC} = 20 dB
Analog Self-interference cancellation power P_{AC}	50 mW
Linear gains of all antennas	10 dBi

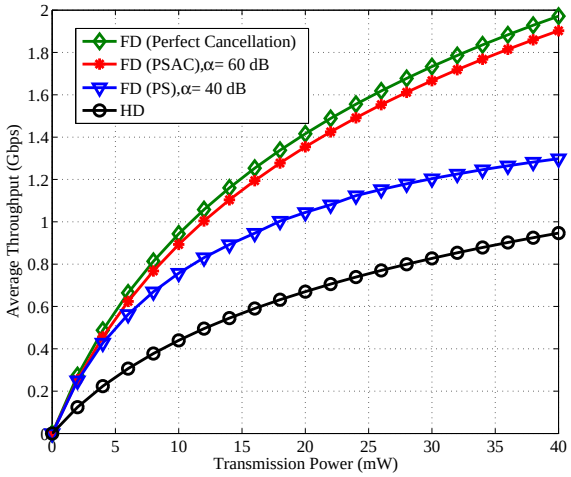

Fig. 2. The average throughputs of the FD (with perfect interference cancellation), FD (PSAC, α = 60 dB), FD (PS, α = 40 dB) and HD relaying.

Fig. 3 shows the average optimal EE performances of FD (PSAC, α = 60 dB), FD (PS, α = 40 dB) and HD under the proposed GC algorithm with given maximum transmission power constraint P_{max}. With given transmission power which is under the maximum transmission power constraint of

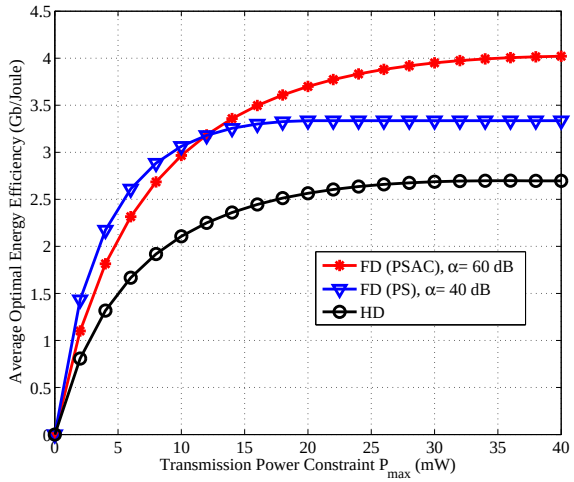

Fig. 3. Average optimal EE performances of FD (PSAC, α = 60 dB), FD (PS, α = 40 dB) and HD relaying.

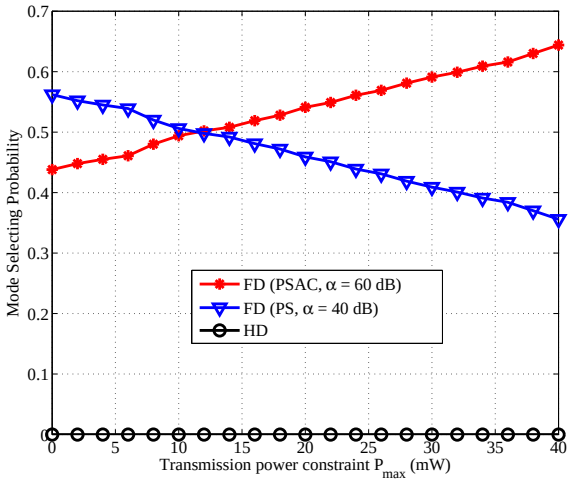

Fig. 4. Probabilities of selecting FD (PSAC, α = 60 dB), FD (PS, α = 40 dB) and HD relaying.

$P_{max} > 12$ mW, FD (PSAC) achieves the highest optimized EE among the three relaying modes, while FD (PS) is the most energy efficient if $P_{max} \leq 12$ mW. By applying the GC algorithm and opportunistic relaying mode selection together, the optimized EE by FD relaying can be up to 1.4 Gb/Joule higher than that of HD relaying. Also, FD (PSAC, α = 60 dB) demonstrates higher average EE than HD across all transmission powers, which verifies the special case in Remark 1. Besides, the value of the average optimal EE of FD (PSAC) is mono-increasing under the transmission power constraint P_{max}, because its EE is a mono-increasing function of the transmission power under the P_{max} constraint. While the EE of FD (PS) is strictly quasi-concave within the given range of transmission power. Therefore, its average optimal EE is unchanged when P_{max} is higher than 22 mW.

Fig. 4 shows the probabilities of selecting FD (PSAC, α = 60 dB), FD (PS, α = 40 dB) and HD, respectively, by applying Algorithm 2. The result is consistent with the result in Fig. 3, that is, FD (PS) is preferable with a relatively low transmission power constraint P_{max}, while FD (PSAC) is preferable with a relatively high P_{max}, in terms of the optimized EE. When P_{max} is low, the critical transmission power $P_s^{\dagger,1}$ in (19) easily exceeds P_{max}. Thus, according to Lemma 1, FD (PS) easily outperforms FD (PSAC) in terms of the optimized EE by the GC algorithm. With the increase of P_{max}, the probability of $P_s^{\dagger,1} < P_{max}$ becomes higher, implying that FD (PSAC) has a higher chance of achieving a higher EE than FD (PS) does. Also, the probability of selecting HD is 0 across all values of P_{max}, showing that FD relaying is always more energy efficient than HD relaying with the simulation setup.

Fig. 5 shows the effect of self-interference cancellation by PS on the probabilities of selecting among the FD (PSAC), FD (PS) and HD modes, by using Algorithm 2. The amount of self-interference canceled by PS, α_{PS}, varies from 20$\sim$70 dB, as the performance of PS is sensitive to nearby environment, while the amount of self-interference cancellation by AC is set to α_{AC} = 20 dB. With the increase of the value of α_{PS}, FD

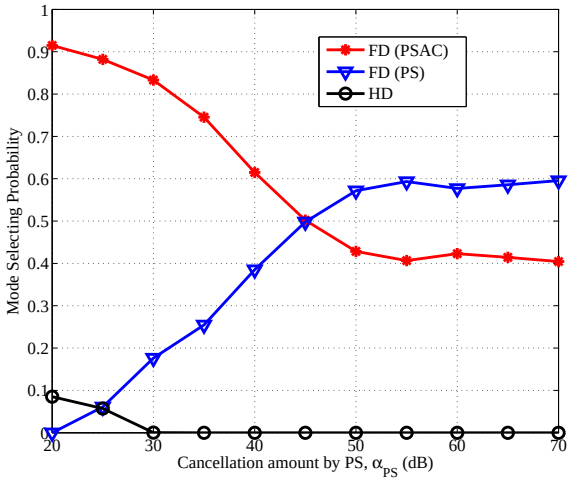

Fig. 5. Probabilities of selecting FD (PSAC), FD (PS) and HD, with the amount of self-interference canceled by AC α_{AC} = 20 dB and the transmission power P_s = 20 mW.

(PS) has a higher chance of achieving a higher optimal EE than FD (PSAC) and HD. In this case, applying AC leads to the decrease of EE, which verifies Remark 3. Only with $\alpha_{PS} < 30$ dB, which occurs rarely [5], HD mode may be selected with a probability of up to 10%, due to highest EE achievable. This is because the throughput of HD is higher than those of FD (PS) and FD (PSAC), or the throughput of HD is lower than that of FD (PSAC) while the crossing transmission power $P_s^{\dagger,2}$ is not achievable under the P_{max} constraint.

Fig. 6 shows the EEs of FDs and HD with drain efficiency set to ω = 25% and 15%, respectively. It is obvious that lower drain efficiency results in lower EEs for all modes. The maximum EE reduction is 1 Gb/Joule when the drain efficiency decreases from 25% to 15%. This is because lower drain efficiency leads to more power being dissipated by PAs. Besides, it can be seen that lower drain efficiency makes FD

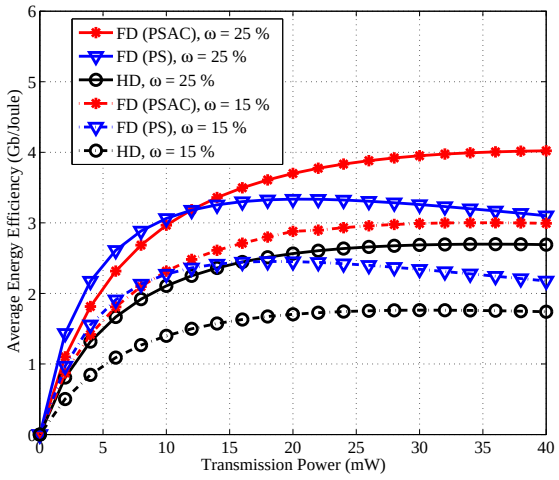

Fig. 6. EE performances of FD (PSAC) and FD (PS), with drain efficiency ω = 25% and 15%.

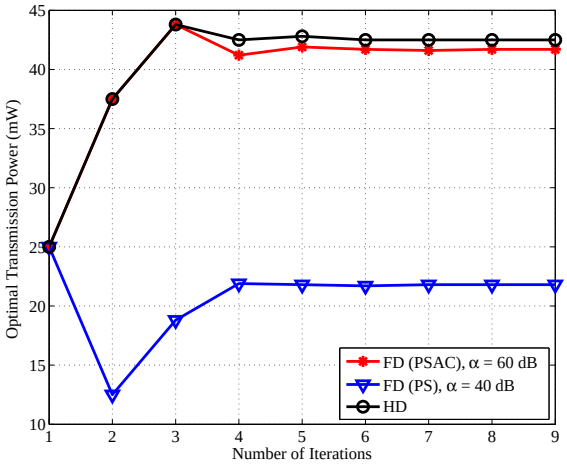

Fig. 8. Convergence behaviors of the proposed GC algorithm for FD (PSAC, α = 60 dB), FD (PS, α = 40 dB) and HD, with maximum transmission power P_{max} = 100 mW.

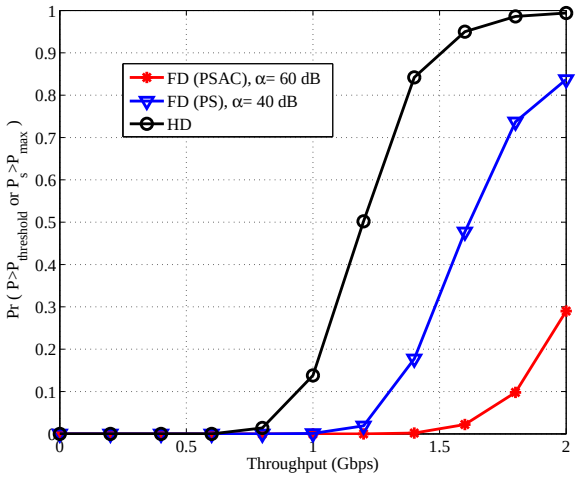

Fig. 7. Outage probabilities of FD (PSAC, α= 60 dB), FD (PS, α= 40 dB) and HD, with total power threshold $P_{threshold}$= 500 mW and transmission power constraint P_{max}= 40 mW.

(PSAC) outperform FD (PS) more easily. With ω=25%, FD (PSAC) outperforms FD (PS) when the transmission power is beyond a threshold of 12 mW, while it is 8 mW with ω=15%. This confirms our finding in Remark 2. High static circuit power has similar effects on EE to low drain efficiency. The results are not shown due to space limit.

Fig. 7 shows the outage probabilities that the total power consumption exceeds a threshold $P_{threshold}$= 500 mW or the transmission power exceeds an upper limit P_{max}= 40 mW. When the throughput is lower than 0.6 Gbps, the outage probabilities of all three relaying modes are 0, implying that low throughput can be easily achieved by all three relaying modes, with low carbon footprint. With the increase of the throughput, the outage probability of HD boosts fast, because HD needs much higher transmission power to pursue high throughput. Therefore, its transmission power or total power consumption easily exceeds the threshold. In particular, for a throughput higher than 1.8 Gbps, the outage probability of HD is nearly 1, implying that HD requires much higher transmission power and total power to achieve a high throughput. For FD (PSAC, α= 60 dB) and FD (PS, α= 40 dB), however, the outage probabilities are lower, which are only 0.1 and 0.75 at 1.8 Gbps, respectively. This confirms that FD relaying is a greener solution for higher speed communication, with more carbon footprint savings.

Fig. 8 shows the convergence behaviors of FD (PSAC), FD (PS) and HD by the GC algorithm under the maximum transmission power constraint P_{max} = 100 mW. Only around 6 iterations are needed in all three cases to achieve the steady states. The optimal transmission power corresponding to the maximized EE is around 42 mW for FD (PSAC) and 43 mW for HD , while it is only around 22 mW for FD (PS). It is because the optimal transmission power is around the value that makes the sum of the PA power and dynamic circuit power comparable with the static circuit power. FD (PSAC) consumes the highest circuit power among three relaying modes, therefore its optimal transmission power needs to be high enough to compensate for the highest circuit power. For HD, its optimal transmission power is also high due to its low achievable throughput resulting in a low dynamic circuit power. Note that if P_{max} is relatively small, *e.g.*, $P_{max} \leq$ 40 mW, the EEs may be mono-increasing in the range of $P_s \in (0, P_{max}]$ as analyzed in Theorem 1. In this case, the transmission power corresponding to the maximum EE is simply equal to P_{max}, and no iteration is needed.

VI. Conclusion

With a full range of power consumption sources considered, we have compared the EE gain regions of FD (PSAC), FD (PS) and HD relaying modes in dual-hop OFDM systems at 60 GHz. It is found that FD (PS) can outperform HD in terms of EE, while FD (PSAC) is even more energy efficient than FD (PS) if the transmission power is higher than a threshold in the feasible range. It is proved that EE is strictly quasi-concave or

mono-increasing with respect to the transmission power under a maximum transmission power constraint. A low-complexity algorithm is proposed to optimize EE by calculating the gradient of EE with respect to the transmission power. Based on the EE optimization and opportunistic relaying mode selection, the average optimal EE of FD relaying is up to 1.4 Gb/Joule higher than that of HD relaying with given transmission power. It is shown that with the same transmission power, the throughput achieved by FD relaying is 1.3∼2 times of that of HD relaying, when the self-interference cancellation amount varies from 40∼60 dB (40 dB can be achieved by PS only with relative ease). It is also shown that with low drain efficiency or high static circuit power, FD (PSAC) is preferable over FD (PS) in terms of EE. This work is general and is applicable to a short-range wireless relay system at any frequency band.

APPENDIX A
PROOF OF THEOREM 1

Hereby we prove the concavity of the EE of FD (PSAC) with respect to the total transmission power P_s (FD (PS) and HD can be seen as special cases). Define $\boldsymbol{B} = \{T_{FD(PSAC)} | T_{FD(PSAC)} \in (0,\infty)\}$ as the set of the overall throughput, while $\boldsymbol{A} = \{P_s | P_s \in (0,\infty)\}$ is the corresponding total transmission power. With a specific mapping function (power allocation method) $f : P_s \xrightarrow{f} T_{FD(PSAC)}$, the total transmission power and the overall throughput is one-to-one mapped ($f : \boldsymbol{A} \xrightarrow{f} \boldsymbol{B}$) and higher transmission power leads to higher throughput. Therefore, if EE $\eta_{FD(PSAC)}$ is strictly quasi-concave with respect to the overall throughput $T_{FD(PSAC)}$, it is also quasi-concave with respect to the total transmission power P_s. The superlevel sets of $\eta_{FD(PSAC)}$ is defined as $S_\Upsilon = \{T_{FD(PSAC)} > 0 | \eta_{FD(PSAC)} > \Upsilon\}$. According to [42], $\eta_{FD(PSAC)}$ is strictly quasi-concave with respect to $T_{FD(PSAC)}$ if S_Υ is strictly convex for any real number Υ. If $\Upsilon < 0$, there is no physical meaning. If $\Upsilon \geq 0$, S_Υ is equivalent to $S_\Upsilon = \{T_{FD(PSAC)} > 0 | \Upsilon(P_s/\omega)\sum_{n=1}^{N}\tilde{\lambda}_n + \Upsilon(P_{c,sta}+P_{AC}) + (\Upsilon\varepsilon - 1)T_{FD(PSAC)} \leq 0\}$. It is known that P_s is strictly convex with respect to $T_{FD(PSAC)}$ given a sufficiently large number of subcarriers [4] [26] and with good self-interference cancellation. The linear part $\Upsilon(P_{c,sta}+P_{AC}) + (\Upsilon\varepsilon - 1)T_{FD(PSAC)}$ is convex (not strictly) with respect to throughput $T_{FD(PSAC)}$. Therefore, the summation $\Upsilon(P_s/\omega)\sum_{n=1}^{N}\tilde{\lambda}_n + \Upsilon(P_{c,sta}+P_{AC}) + (\Upsilon\varepsilon - 1)T_{FD(PSAC)}$ is strictly convex with respect to throughput $T_{FD(PSAC)}$. In conclusion, $\eta_{FD(PSAC)}$ is strictly quasi-concave with respect to $T_{FD(PSAC)}$, and is strictly quasi-concave with respect to P_s. Under a small maximum transmission power constraint P_{max}, $\eta_{FD(PSAC)}$ may be mono-increasing with respect to the total transmission power P_s.

APPENDIX B
DERIVATIVE CALCULATION OF EE WITH RESPECT TO THE TOTAL TRANSMISSION POWER

Hereby we take FD (PSAC) as example to show the derivative calculation of EE with respect to the total transmission power (FD (PS) and HD can be seen as special cases). For the strictly-continuous function $\eta_{FD(PSAC)}$ in the region $P_s \in (0, P_{max}]$, the limit of the difference quotient when ΔP_s approaches zero, if existing, should represent the slope of the tangent line to (P_s, $\eta_{FD(PSAC)}$), which is calculated as

$$\begin{aligned}&\frac{\partial \eta_{FD(PSAC)}}{\partial P_s}|_{P_s} \\ &= \lim_{\Delta P_s \to 0} \frac{\eta_{FD(PSAC)}(P_s+\Delta P_s) - \eta_{FD(PSAC)}(P_s)}{\Delta P_s}.\end{aligned} \tag{22}$$

With a minimal increment ΔP_s that approaches 0, we can get the values of $\eta_{FD(PSAC)}(P_s + \Delta P_s)$ and $\eta_{FD(PSAC)}(P_s)$, respectively. Substituting the two terms into (22), $\partial\eta_{FD(PSAC)}/\partial P_s$ can be found. Therefore, calculating $\frac{\partial \eta}{\partial P_s}$ can be transferred into calculating $\eta_{FD(PSAC)}$ at transmission powers P_s and $P_s + \Delta P_s$.

APPENDIX C
EE GAIN REGIONS AMONG FD (PSAC), FD (PS) AND HD

A. EE Gain Region between FD (PSAC) and FD (PS)

The difference between the EEs of FD (PSAC) and FD (PS) is calculated as

$$\begin{aligned}&\eta_{FD(PSAC)} - \eta_{FD(PS)} = \\ &\frac{\left(\frac{P_s}{\omega}\sum_{n=1}^{N}\tilde{\lambda}_n + P_{c,sta}\right)\left(\frac{T_{FD(PSAC)}}{T_{FD(PS)}} - 1\right) - P_{AC}}{T_{FD(PS)}\left(\frac{P_s}{\omega}\sum_{n=1}^{N}\tilde{\lambda}_n + \varepsilon T_{FD(PSAC)} + P_{c,sta} + P_{AC}\right)} \\ &\times \frac{1}{\left(\frac{P_s}{\omega}\sum_{n=1}^{N}\tilde{\lambda}_n + \varepsilon T_{FD(PS)} + P_{c,sta}\right)},\end{aligned} \tag{23}$$

where $T_{FD(PSAC)}$ and $T_{FD(PS)}$ represent the throughputs achieved by FD (PSAC) and FD (PS), respectively. Obviously, the sign of (23) is the same as the sign of its numerator.

B. EE Gain Region between FD (PSAC) and HD

The difference between the EEs of FD (PSAC) and HD is calculated as

$$\begin{aligned}&\eta_{FD(PSAC)} - \eta_{HD} = \\ &\frac{\left(\frac{P_s}{\omega}\sum_{n=1}^{N}\tilde{\lambda}_n + P_{c,sta}\right)\left(\frac{T_{FD(PSAC)}}{T_{HD}} - 1\right) - P_{AC}}{T_{HD}\left(\frac{P_s}{\omega}\sum_{n=1}^{N}\tilde{\lambda}_n + \varepsilon T_{FD(PSAC)} + P_{c,sta} + P_{AC}\right)} \\ &\times \frac{1}{\left(\frac{P_s}{\omega}\sum_{n=1}^{N}\tilde{\lambda}_n + \varepsilon T_{HD} + P_{c,sta}\right)},\end{aligned} \tag{24}$$

where $T_{FD(PSAC)}$ and T_{HD} are throughputs achieved by FD (PSAC) and HD, respectively.

Specially, with near-perfect self-interference cancellation, the throughput of FD (PSAC) is nearly twice as high as that of HD. Hence, (24) reduces to

$$\begin{aligned}&\eta_{FD(PSAC)} - \eta_{HD} = \\ &\frac{\left(\frac{P_s}{\omega}\sum_{n=1}^{N}\tilde{\lambda}_n + P_{c,sta}\right) - P_{AC}}{T_{HD}\left(\frac{P_s}{\omega}\sum_{n=1}^{N}\tilde{\lambda}_n + \varepsilon T_{FD(PSAC)} + P_{c,sta} + P_{AC}\right)} \\ &\times \frac{1}{\left(\frac{P_s}{\omega}\sum_{n=1}^{N}\tilde{\lambda}_n + \varepsilon T_{HD} + P_{c,sta}\right)}.\end{aligned} \tag{25}$$

C. EE Gain Region between FD (PS) and HD

FD (PS) uses antenna shielding or directional antenna to mitigate self-interference, and therefore it does not consume additional power on self-interference cancellation. With the same transmission power, the EE difference between FD (PS) and HD is calculated as

$$\begin{aligned}&\eta_{FD(PS)} - \eta_{HD} = \\ &\frac{\left(\frac{P_s}{\omega}\sum_{n=1}^{N}\tilde{\lambda}_n + P_{c,sta}\right)\left(T_{FD(PS)} - T_{HD}\right)}{T_{HD}\left(\frac{P_s}{\omega}\sum_{n=1}^{N}\tilde{\lambda}_n + \varepsilon T_{FD(PS)} + P_{c,sta}\right)} \\ &\times \frac{1}{\left(\frac{P_s}{\omega}\sum_{n=1}^{N}\tilde{\lambda}_n + \varepsilon T_{HD} + P_{c,sta}\right)},\end{aligned} \tag{26}$$

where $T_{FD(PS)}$ and T_{HD} are the throughputs achieved by FD (PS) and HD, respectively. The sign of (26) is the same as the sign of $T_{FD(PS)} - T_{HD}$, *i.e.*, FD (PS) is more energy efficient than HD if FD (PS) achieves a higher throughput than HD.

REFERENCES

[1] J. Qiao, L. X. Cai, X. Shen and J. W. Mark, "Enabling multi-hop concurrent transmissions in 60 GHz wireless personal area networks," *IEEE Trans. Wireless Commun.*, vol. 10, no. 11, pp. 3824-3833, Nov. 2011.

[2] T. S. Rappaport, S. Sun, R. Mayzus, H. Zhao, Y. Azar, K. Wang, G. N. Wong, J. K. Schulz, M. Samimi and F. Gutierrez, "Millimeter wave mobile communications for 5G cellular: It will work!" *IEEE Access*, vol. 1, pp. 335-349, May 2013.

[3] S. Singh, F. Ziliotto, U. Madhow, E. M. Belding and M. Rodwell, "Blockage and directivity in 60 GHz wireless personal area network: From cross-layer model to multi-hop MAC design," *IEEE J. Sel. Areas Commun.*, vol. 27, no. 8, pp. 1700-1713, Oct. 2009.

[4] D. W. K. Ng, E. S. Lo and R. Schober, "Dynamic resource allocation in MIMO-OFDMA systems with full-duplex and hybrid relaying," *IEEE Trans. Commun.*, vol. 60, no. 5, pp. 1291-1304, May 2012.

[5] E. Everett, A, Sahai and A. Sabharwal, "Passive self-interference suppression for full-duplex infrastructure nodes," *IEEE Trans. Wireless Commun.*, vol. 13, no. 2, pp. 680-694, Feb. 2014.

[6] C. Marcu, D. Chowdhury, C. Thakkar, J. D. Park, L. K. Kong, M. Tabesh, Y. Wang, B. Afshar, A. Gupta, A. Arbabian, S. Gambini, R. Zamani, E.Alon and A. M. Niknejad, "A 90 nm CMOS low-power 60 GHz transceiver with integrated baseband circuitry," *IEEE J. Solid-State Circuit*, vol. 44, no. 12, pp. 3434-3447, Dec. 2009.

[7] R. Bolla, R. Bruschi, F. Davoli and F. Cucchietti, "Energy efficiency in the future internet: A survey of existing approaches and trends in energy-aware fixed network infrastructures," *IEEE Commun. Surveys Tut.*, vol. 13, no. 2, pp. 223-244, Jul. 2011.

[8] D. Sabella, A. D. Domenico, E. Katranaras, M. A. Imran, M. D. Girolamo, U. Salim, M. Lalam, K. Samdanis and A. Maeder, "Energy efficiency benefits of ran-as-a-service concept for a cloud-based 5G mobile network infrastructure," *IEEE Access*, vol. 2, pp. 1586-1597, Dec. 2014.

[9] EARTH Project. D2.3 Energy efficiency analysis of the reference systems, areas of improvements and target breakdown. [Online]. Available: http://www.ict-earth.eu/publications/publications.html

[10] A. Sabharwal, P. Schniter, D. Guo, D. W. Bliss, S. Rangarajan and R. Wichman, "In-band full-duplex wireless: challenges and opportunities," *IEEE J. Sel. Areas Commun.*, vol. 32, no. 9, pp. 1637-1652, Sep. 2014.

[11] M. Duarte, A. Sabharwal, V. Aggarwal, R. Jana, K. K. Ramakrishnan, C. W. Rice and N. K. Shankaranarayanan, "Design and characterization of a full-duplex multiantenna system for WiFi networks," *IEEE Trans. Veh. Tech.*, vol. 63, no. 3, pp. 1160-1177, Mar. 2014.

[12] V. Syrjala, M. Valkama, L. Anttila, T. Riihonen and D. Korpi, "Analysis of oscillator phase-noise effects on self-interference cancellation in full-duplex OFDM radio transceivers," *IEEE Trans. Wireless Commun.*, vol. 13, no. 06, pp. 2977-2990, Jun. 2014.

[13] Z. He, S. Shao, Y. Shen. C. Qing and Y. Tang, "Performance analysis of RF self-Interference cancellation in full-Duplex wireless communiations," *IEEE Wireless Lett.*, vol. 3, no. 4, pp. 405-408, Aug. 2014.

[14] M. Jain, J. I. Choi, T. Kim, D. Bharadia, S. Seth, K. Srinivasan, P. Levis, S. Katti and P. Sinha, "Practical, real-time, full duplex wireless," in *Proc. ACM MobiCom'10*, New York, USA, Sep. 2010.

[15] M. Duarte, C. Dick and A. Rshulosh, "Experiment-driven characterization of full-duplex wireless systems," *IEEE Trans. Wireless Commun.*, vol. 11, no. 12, pp. 4296-4307, Dec. 2012.

[16] A. Sahai, G. Pate and A. Sabharwal, "Pushing the limits of full-duplex: Design and real-time implementation," Rice Univ., Houston, USA, Tech. Rep. TREE 1104, Jul. 2011, arXiv:1311.6247v1[cs.IT].

[17] G. Liu, F. R. Yu, H. Ji, V. C. M. Leung and X. Li, "In-band full-duplex relaying: A survey, research issues and challenges," *IEEE Commun. Surveys Tuts.*, 2015. 2394324, Jan. 2015.

[18] J. Lee and O. S. Shin, "Full-duplex relay based on distributed beamforming in multiuser MIMO systems," *IEEE Trans. Veh. Tech.*, vol. 62, no. 4, pp. 1855-1860, May 2013.

[19] S. Huberman and T. L. Ngoc, "MIMO Full-Duplex Precoding: A joint beamforming and self-interference cancellation srtucture," *IEEE Trans. Wireless Commun.*, vol. 14, no. 4, pp. 2205-2217, Apr. 2015.

[20] E. Ahmed, A. M. Eltawil and A. Sabharwal, "Rate gain region and design tradeoffs for full-duplex wireless communications," *IEEE Trans. Wireless Commun.*, vol. 12, no. 7, pp. 3556-3565, Jul. 2013.

[21] W. Li, J. Lillegerg and K. Rikkinen, "On rate region analysis of half-and full-duplex OFDM communication links," *IEEE J. Sel. Areas Commun.*, vol. 32, no. 9, pp. 1688-1698, Sep. 2014.

[22] L. Dong, S. Sun, X. Zhu and Y. K. Chia, "Power efficient 60 GHz wireless communication networks with relays," in *Proc. IEEE PIMRC' 13*, London, UK, Sep. 2013.

[23] G. Miao, N. Himayat and G. Y. Li, "Energy-efficient link adaptation in frequency-selective channels," *IEEE Trans. Commun.*, vol. 58, no. 2, pp. 545-554, Feb. 2010.

[24] S. Cui, A. J. Goldsmith and A. Bahai, "Energy-efficiency of MIMO and cooperative MIMO techniques in sensor networks," *IEEE J. Sel. Areas Commun.*, vol. 22, no. 6, pp. 1089-1098, Aug. 2004.

[25] S. Cui, A. J. Goldsmith and A. Bahai, "Energy-constrained modulation optimization," *IEEE Trans. Wireless Commun.*, vol. 4, no. 5, pp. 2349-2360, Sep. 2005.

[26] C. Xiong, G. Y. Li, S. Zhang, Y. Chen and S. Xu, "Energy-and spectral-efficiency tradeoff in downlink OFDMA networks," *IEEE Wireless Commun. Lett.*, vol. 10, no. 11, pp. 3874-3886, Nov. 2011.

[27] Y. Li, M. Reisslein and C. Chakrabarti, "Energy-efficient video transmission over a wireless link," *IEEE Trans. Veh. Tech.*, vol. 58, no. 3, pp. 1229-1244, Mar. 2009.

[28] O. Waqar, M. A. Imran, M. Dianati and R. Tafazolli, "Energy consumption analysis and optimization of BER-constrained amplify-and-forward relay networks," *IEEE Trans. Veh. Tech.*, vol. 63, no. 3, pp. 1256-1269, Mar. 2014.

[29] D. Quintas and V. Friderikos, "Energy efficient relaying within a cell: multi path versus shortest path routing," in *Proc. IEEE INFOCOM'10*, San Diego, USA, Mar. 2010.

[30] Q. Liu, Z. Wei, X. Ma and G. T. Zhou, "Designing peak power constrained amplify-and-forward relay networks with cooperative diversity," *IEEE Trans. Wireless Commun.*, vol. 11, no. 5, pp. 1733-1743, May 2014.

[31] V. K. Sakarellos, D. Skraparlis, A. D. Panagopoulos and J. D. Kanellopoulos, "Optimum placement of radio relays in millimeter-wave wireless dual-hop networks," *IEEE Trans. Wireless Commun.*, vol. 51, no. 2, pp. 190-199, Apr. 2009.

[32] D. Dardari and V. Tralli, "High-speed indoor wireless communications at 60 GHz with coded OFDM," *IEEE Trans. Commun.*, vol. 47, no. 11, pp. 1709-1721, Nov. 1999.

[33] N. Moraitis and P. Constantinou, "Measurements and characterization of wideband indoor radio channel at 60 GHz," *IEEE Trans. Commun.*, vol. 5, no. 4, pp. 880–889, Apr. 2006.

[34] T. S. Rappaport, R. W. Heath, R. C. Daniels and J. N. Murdock, "Millimeter Wave Wireless Communications," *Prentice Hall*, 2015.

[35] T. Riihonen, S. Werner and R. Wichman, "Hybrid full-duplex/half-duplex relaying with transmit power adaptation," *IEEE Trans. Wireless Commun.*, vol. 10, no. 9, pp. 3074-3085, Sep. 2011.

[36] A. Siligaris, Y. Hamada, C. Mount, C. Raynaud, B. Martineau, N. Deparis, N. Rolland, M. Fukaishi and P. Vincent, "A 60 GHz power amplifier with 14.5 dBm saturation power and 25% peak PAE in CMOS 65 NM SOI," *IEEE J. Solid-State Circuit*, vol. 45, no. 7, pp. 1286-1294, Jul. 2010.

[37] P. Grover, K. Woyach and A. Sahai, "Towards a communication theoretic understanding of system-Level power consumption," *IEEE J. Sel. Areas Commun.*, vol. 29, no. 8, pp. 1744-1755, Sep. 2011.

[38] EARTH Project, D3.4 Advanced radio interface technologies for 4G systems ARTIST4G. [Online]. Available: https://ict-artist4g.eu
[39] O. Arnold, F. Richter, G. P. Fettweis and O. Blume, "Power consumption modeling of different base station types in heterogeneous cellular networks," in *Proc. ICT MobileSummit'10*, Florence, Italy, Jun. 2010.
[40] K. Yamamoto, K. Haneda, H. Murata and S. Yoshida,"Optimal transmission scheduling for a hybrid of full- and half-duplex relaying," *IEEE Commun Lett.*, vol. 15, no. 3, pp. 305-307, Sep. 2011.
[41] S. Geng, J. Kivinen, X. Zhao and P. Vainikainen, "Millimeter-wave propagation channel characterization for short-range wireless communications," *IEEE Trans. Wireless Commun.*, vol. 58, no. 1, pp. 3-12, Jan. 2009.
[42] S. Boyd and L. Vandenberghe, "Convex Optimization," *Cambridge University Press*, 2004.

Zhongxiang Wei received the M.S. degree in 2013, in Information and Communication Engineering from Chongqing University of Posts and Telecommunications, Chongqing, China. He is currently a Ph.D. candidate at the Department of Electrical Engineering and Electronics, the University of Liverpool. His research interests include green communications, full-duplex, millimeter-wave communications, wireless resource allocation and algorithm design.

Xu Zhu (S'02-M'03-SM'12) received the BEng degree (with the first class honors) from Huazhong University of Science and Technology, Wuhan, China, in 1999, and the PhD degree from the Hong Kong University of Science and Technology, Hong Kong, in 2003. Since 2003, she has been with the Department of Electrical Engineering and Electronics, the University of Liverpool, Liverpool, UK, where she is currently a Senior Lecturer. Dr. Zhu has over 130 peer-reviewed publications on communications and signal processing. She is an Editor for the IEEE Transactions on Wireless Communications, and has served as a Guest Editor for several international journals. She has been involved in a large number of conference organizing committees, *e.g.,* as Symposium Chair of the IEEE ICC 2016. Her research interests include MIMO, equalization, resource allocation, cognitive radio, smart grid communications *etc*.

Sumei Sun (SM'12) received the B.Sc, M.Eng, and Ph.D degrees from Peking University, China, Nanyang Technological University, and National University of Singapore, Singapore, respectively. She has been with Institute for Infocomm Research (I^2R) since 1995, where she is currently Head of the Cognitive Communications Technology Department. Dr. Sun has been actively organizing international conferences, *e.g.*, as Executive Co-Chair of Globecom 2017, Symposium Co-Chair of ICC 2015 and 2016, Publicity Co-Chair of PIMRC 2015, Track Co-Chair of VTC 2012 Spring and 2014 Spring and TPC Co-Chair of the IEEE ICCS 2010 and 2014. She is an Editor for IEEE Transactions on Vehicular Technology (TVT) and IEEE Wireless Communication Letters. She was recognized as the "**Top15 Outstanding Editors**" (2014) and "**Top Associate Editor**" (2012 and 2013) by TVT. She is a distinguished lecturer of the IEEE Vehicular Technology Society 2014-2016, a co-recipient of the 16^{th} PIMRC Best Paper Award, and Distinguished Visiting Fellow of the Royal Academy of Engineering, UK, in 2014.

Yi Huang (S'91-M'96-SM'06) received the DPhil in Communications from the University of Oxford, UK in 1994. He has been conducting research in wireless communications, applied electromagnetics, radar and antennas since 1987. His experience includes 3 years spent with NRIET (China) as a Radar Engineer and various periods with the Universities of Birmingham, Oxford, and Essex at the UK. He worked as a Research Fellow at British Telecom Labs in 1994, and then joined the University of Liverpool, UK in 1995, where he is now a full Professor and Deputy Head of the Department of Electrical Engineering and Electronics. Dr. Huang has published over 300 refereed papers, received many research grants from various funding bodies and acted as consultant for various companies. He has been a keynote/invited speaker and organizer of many conferences and workshops (*e.g.*, WiCom2010, IEEE iWAT 2010 and LAPC2012). He is the Editor-in-Chief of Wireless Engineering and Technology and has been an Editor or Guest Editor for four international journals. He is a UK national representative of EU COST-IC1102 and Executive Committee Member and Fellow of the IET.

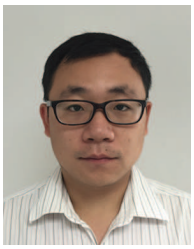

Linhao Dong (S'13-M'15) received a dual BEng degree from Dalian Nationalities University, China, and Glyndwr University, UK, in 2009, and the PhD degree from the University of Liverpool, UK, in 2013. He joined the School of Aerospace Engineering, Tsinghua University as a postdoctoral researcher in April 2014. His research interests include green communications, wireless resource allocation, cooperative networks, millimeter-wave communications, and wireless multimedia communications. He served as the organization chair of the QoEWC Workshop 2015 and the TPC member of the IEEE ICCI*CC 2015.

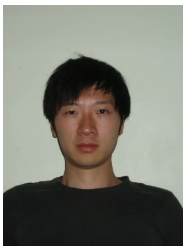

Yufei Jiang (S'12-M'14) received the Ph.D. degree in Wireless Communications and Signal Processing from the University of Liverpool, Liverpool, U.K, in 2014. Since then, he has been with the Department of Electrical and Electronic Engineering as a postdoctoral researcher of the University of Liverpool. His research interests include MIMO, CoMP communication, full-duplex, OFDM, synchronization and blind source separation.